Three-Dimensional Time-Dependent Wavepacket Calculation of the Transition State Resonances for MuH2 and MuD2: Resonance Energies and Widths

ARTICLE *in* THE JOURNAL OF PHYSICAL CHEMISTRY · AUGUST 1996

Impact Factor: 2.78 · DOI: 10.1021/jp9610372

2 AUTHORS:

Hyeong G Yu
Seoul National University
169 PUBLICATIONS **1,531** CITATIONS
SEE PROFILE

Antonio J. C. Varandas
University of Coimbra
382 PUBLICATIONS **6,806** CITATIONS
SEE PROFILE

Three-Dimensional Time-Dependent Wavepacket Calculation of the Transition State Resonances for MuH_2 and MuD_2: Resonance Energies and Widths

H. G. Yu and A. J. C. Varandas*

Departamento de Química, Universidade de Coimbra, 3049 Coimbra Codex, Portugal

Received: April 3, 1996; In Final Form: June 10, 1996[⊗]

The transition state resonances of Mu + H_2 and Mu + D_2 collisions are investigated on the accurate DMBE potential energy surface for H_3 using a three-dimensional (3D) time-dependent quantum-mechanical method for total angular momentum $J = 0$. The discrete variable representation−finite basis representation (DVR−FBR) transform method is used to describe the dynamics in the bending coordinate, while the two stretching coordinates are treated by a sine fast Fourier transform (FFT) technique. The time propagation of the wavepacket is carried out using the Feit−Fleck split operator algorithm. For both systems, the progressions of the resonance states in 3D are the same as in 2D. Compared with the 2D results, their lifetimes tend to be shorter.

Introduction

Transition state resonances in bimolecular reactive collisions have received considerable attention in recent years.[1−8] The prototypical chemical reaction H + H_2 has been in this context particularly well studied.[9−18] For this system, several short-lifetime resonances at energies between 0.54 and 4.63 eV have been discovered in both two- and three-dimensional (2D and 3D, respectively) quantum mechanical calculations. Moreover, most 3D resonance energies have been shown to be consistently related to the collinear resonance energies by adding to the latter the nearly separable degenerate bends.

Although there have been many experimental measurements[19−21] and theoretical calculations[22−27] for the isotopic reactions Mu + H_2 and Mu + D_2, all focused on studies of reaction rates. Thus, much less is known about their transition state resonances. In a previous paper,[28] we reported a collinear calculation of transition state resonances for the Mu + H_2 and Mu + D_2 systems using the accurate DMBE potential energy surface[29] for H_3 and the split operator algorithm proposed by Feit and Fleck[30,31] to propagate the wavepacket. In that work,[28] we reported 12 transition state resonances for Mu + H_2 and 16 for Mu + D_2. Compared to their isotope analogues H + H_2 and D + H_2, which have been studied in detail by Skodje and co-workers,[15−18] it has been found that the muonic systems show a distinct resonance pattern. These new features of the transition state resonance for the muonic systems prompted us to carry out the 3D calculations reported in the present work. Similarly to the H + H_2[16] case, the resonance structure predicted in our collinear calculations for the title systems will be shown to persist in 3D.

The structure of this work is as follows. After a brief description of the methodology, the results and discussion are presented, followed by a brief summary.

Methodology

We seek a description of the Mu + A_2 (A = H or D) transition state dynamics in terms of a quantum-mechanical wavepacket $\psi(r, R, \theta, t)$, which is calculated by solving the time-dependent Schrödinger equation

$$(i\hbar)[\partial\psi(r, R, \theta, t)/\partial t] = H\psi(r, R, \theta, t) \tag{1}$$

where (r, R, θ) are the usual Jacobi coordinates. For total angular momentum $J = 0$, the interaction Hamiltonian can be written as[32]

$$H = K_r + K_\theta + V(r, R, \theta) \tag{2}$$

where

$$K_r = -\frac{\hbar^2}{2\mu}\frac{\partial^2}{\partial r^2} - \frac{\hbar^2}{2m}\frac{\partial^2}{\partial R^2} \tag{3}$$

$$K_\theta = -\frac{\hbar^2}{2I}\frac{1}{\sin\theta}\frac{\partial}{\partial\theta}[\sin\theta(\partial/\partial\theta)] \tag{4}$$

with μ being the reduced mass of A_2, m the reduced mass of Mu + A_2, $I = m\mu r^2R^2/(\mu r^2 + mR^2)$ the moment of inertia, and $V(r, R, \theta)$ the H_3 DMBE potential energy surface.[29]

Following our previous collinear study,[28] the initial wave function $\psi(r, R, \theta, t = 0)$ has been taken as a Gaussian wavepacket in terms of the MuA and AA bond distances and the Jacobi angle θ

$$\psi(r, R, \theta, t=0) = N \exp\left\{-\frac{[(r_{\mathrm{MuA}} - r_0) + (r_{\mathrm{AA}} - r_0)]^2}{8\delta_1^2} - \frac{[(r_{\mathrm{MuA}} - r_0) - (r_{\mathrm{AA}} - r_0)]^2}{2\delta_2^2}\right\} \times \left\{\exp\left[-\frac{(\theta - \theta_0)^2}{2\delta_\theta^2}\right] + \exp\left[-\frac{(\theta - \pi + \theta_0)^2}{2\delta_\theta^2}\right]\right\} \tag{5}$$

and then placed in the vicinity of the saddle point of the H_3 potential energy surface using a 3D discrete grid; r_0 and θ_0 specify the initial position of the wavepacket, and δ_i ($i = 1, 2, \theta$) specifies the width parameters. Such a grid includes a 2D uniform rectangular grid of dimension 128 × 128 used to represent the wavefunction in (r, R) coordinates and a 1D grid of dimension 29 in the θ coordinate; this consists of the quadrature points (the corresponding weights are denoted ω_α) of a 29-point Gauss−Legendre quadrature. The discrete variable representation (DVR) wave function ψ_{DVR} has then been

[⊗] Abstract published in *Advance ACS Abstracts,* August 1, 1996.

S0022-3654(96)01037-4 CCC: $12.00

obtained by multiplying the initial wave function in the coordinate space with a factor of $\omega_\alpha^{1/2}$. Finally, the mixed grid−finite basis representation (FBR) wave function ψ_{FBR} has been defined through the unitary transformation[33]

$$\psi_{FBR} = \mathbf{T}\psi_{DVR} \tag{6}$$

where $\boldsymbol{T}$ is a unitary matrix defined by

$$T_{j\alpha} = \omega_\alpha^{1/2}\varphi_j(\cos\theta_\alpha) \tag{7}$$

with θ_α being the quadrature point, ω_α the weights of the underlying Gauss−Legendre quadrature, and $\varphi_j(\cos\theta)$ the orthonormal Legendre polynomial, which is the eigenfunction of the angular momentum operator. It should be noted from eq 5 that the initial wavefunction $\psi(r, R, \theta, t = 0)$ is symmetric with respect to permutation of the Mu−A and A−A bond distances and shows the proper C_{2v} symmetry with respect to the Jacobi angle θ.

To propagate the wavepacket, we have used the split-operator algorithm described by Feit and Fleck.[30,31,34] For a short time step Δt, the wavefunction $\psi_{FBR}(t_0 + \Delta t)$ can be written as

$$\psi_{FBR}(t_0 + \Delta t) \approx e^{-iK_r\Delta t/2\hbar}e^{-iK_\theta\Delta t/2\hbar}e^{-iV\Delta t/\hbar}e^{-iK_\theta\Delta t/2\hbar}e^{-iK_r\Delta t/2\hbar}\psi_{FBR}(t_0) \tag{8}$$

where K_r and K_θ are the operators defined in eqs 3 and 4 and **V** is the potential energy matrix operator which includes the absorbing (negative imaginary) potentials[35] (NIPs) to prevent reflections of the wavepacket from the edges of the grid; this approach has also been adopted in our previous[28] collinear study. The evolution of the spatial kinetic operators has been carried out using a sine fast Fourier transform technique such that the singularity at $R = 0$ is surpressed. Since the angular momentum operators are diagonal in this mixed grid−basis set representation, they can easily be propagated. However, because **V** is nondiagonal in FBR, the propagations of the potential energy operator have been done with the help of the FBR−DVR transformation in eq 6.

The autocorrelation function

$$C(t) = \langle\psi(0)|\psi(t)\rangle \tag{9}$$

is computed at each time step, and the Fourier transform of $C(t)$ is carried out to generate the pseudo-spectral intensity

$$I(E) \sim \int_{-\infty}^{+\infty} C(t)e^{iEt/\hbar}\,dt \tag{10}$$

The resonance energies E_n and the lifetimes τ_n can be extracted from the strong peak positions and widths in the spectrum by using a nonlinear least-squares fitting of $I(E)$ to a sum of Lorentzians. In practice, the filtered half-spectrum

$$J(E) \sim \left|\int_0^{\infty} C(t)W(t)e^{iEt/\hbar}\,dt\right|^2 \tag{11}$$

is generally more effective than $I(E)$ in reducing the contributions from the background (see also ref 14); $W(t)$ is the normalized Hanning window function.[36] Moreover, we have used the Prony method as modified by Gray[37,38] as a supplementary technique to determine the resonance energies and widths from the autocorrelation function.

Finally, we mention a simple and useful scheme proposed by Engel.[39] It states that, for time-independent Hamiltonian operators and real initial wavepackets, the autocorrelation function for time $2t$ can be constructed from the intermediate wavepacket at time t as

$$C(2t) = \langle\psi^*(t)|\psi(t)\rangle \tag{12}$$

Thus, this techqnique allows the computation time for the calculation of the autocorrelation function to be reduced by a factor of 2. The absolute accuracy of $C(t)$ has been checked in the present study to be better than 10^{-8} with respect to the influence of the NIPs and numerical errors.

Results and Discussion

For the Mu + H_2 system, we have propagated five wavepackets having different initial positions and other parameters. One of these has been located at the linear configuration $r_{MuH} = r_{HH} = 3.10a_0$, with an angular Gaussian width of $\delta_\theta = 0.25$ rad; the spatial Gaussian widths are $\delta_1 = 1.0a_0$ and $\delta_2 = 0.45a_0$ for the symmetric and asymmetric bond stretching coordinates, respectively. Thus, it is a very broad wavepacket in the symmetric stretch coordinate with low bend excitation. Its average energy has been calculated to be 3.223 eV. This wavepacket has been propagated during 220 fs, which has been found sufficient to converge the spectrum.

The 3D transition state spectrum obtained from the above initial wavepacket is shown in Figure 1. For comparison, the complete transition state spectrum calculated[28] for the collinear Mu + H_2 problem is also given in the upper pannel of Figure 1. It can be seen that the progressions of both barrier and conventional resonances are the same in 2D and 3D, except for the two highest states. By introducing a small shift in the frequency toward high energies due to the bend zero-point energy, we have located the zero-bend resonance positions which correspond to the collinear resonance states. The results are presented in Table 1. We note that the energy shift tends to decrease with increasing energy, while the resonance lifetimes are seen to be smaller in the 3D case. Thus, transition state resonances tend to become somewhat unstabilized with increasing dimensionality due to having more degrees of freedom to decay. In addition, we have observed two peaks at 3.944 and 4.404 eV in the 3D collisions, which correspond to the peaks at 3.906 and 4.383 eV in the collinear study[28] in the same order. These resonances have been assigned as "mixed" resonance states in our previous work.[28] It appears that there is an unknown dynamical structure for the Mu + H_2 system, which has not been observed for H + H_2[14,15] and D + H_2.[17] Many bend excited resonances are also apparent in Figure 1, which could not be assigned.

The resonance energies and widths can be determined through a nonlinear least-squares fitting procedure using a sum of Lorentzians. The calculated values are summarized in Table 2. These resonances have been carefully identified by varying the initial wavepacket and using the Prony method as modified by Gray[37,38] to fit the autocorrelation function $C(t)$ to a sum of complex exponentials in time. In particular, for the high-energy resonances, their energies can be well located in terms of the half-spectrum filtered by the Hanning window function. As shown in Figure 2, this half-spectrum is almost noise free. Thus, the accuracy of resonance energies is about 0.005 eV, while the uncertainty of lifetime may be as much as 20%.

Similarly to the Mu + H_2 system, we have propagated four symmetric Gaussian wavepackets for the Mu + D_2 system. The calculated resonance energies and lifetimes are listed in Table 2, while a comparison of the 3D zero-bend resonance states with the 2D ones is given in Table 3. As for the 2D collisions, three progressions are apparent in the resonances calculated from the 3D study of the Mu + D_2 reaction. However, the energy shifts of the zero-bend resonances are not a monotonous function

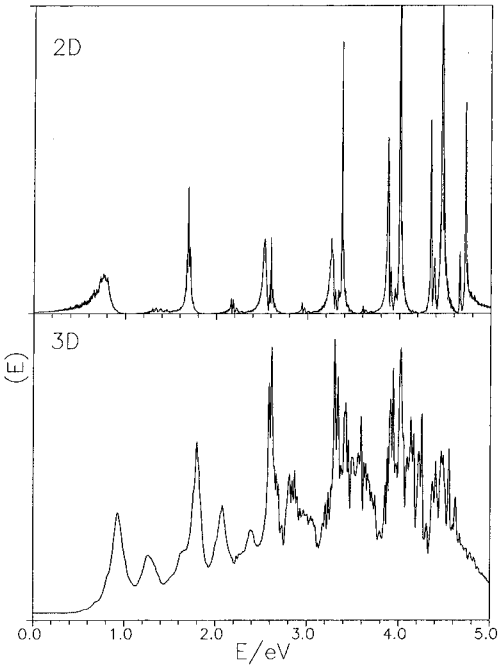

Figure 1. Transition state spectra $I(E)$ for the Mu + H_2 system: two-dimensional (2D) results and three-dimensional (3D) results at the total angular momentum $J = 0$.

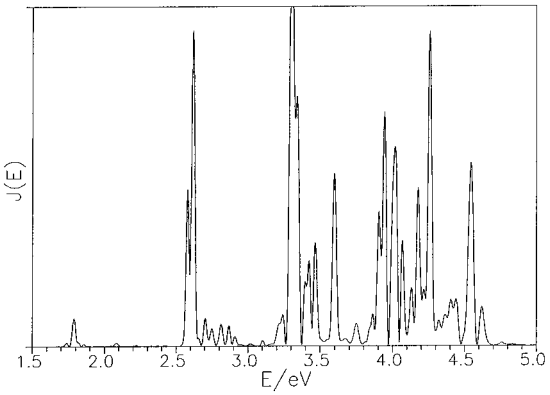

Figure 2. Transition state spectra $J(E)$ for the Mu + H_2 system obtained after the spectrum $I(E)$ of Figure 1 was filtered through a Hanning window function.

TABLE 1: Calculated Energies E_n (eV) and Lifetimes τ_n (fs) of the Transition State Resonances for the Mu + H_2 Collisions: Two-Dimensional Results (2D) (Taken from Ref 28), Zero-Bend Three-Dimensional Results (3D), and Difference ΔE between the 3D and 2D Energies

E_n^{2D}	τ_n^{2D}	E_n^{3D}	τ_n^{3D}	ΔE
0.778	5.5	0.924	5.6	0.146
1.691	50	1.788	6.9	0.097
2.529	16	2.585	18	0.056
2.601	90	2.618	23	0.017
3.266	15	3.305	30	0.039
3.375	93	3.404	22	0.029
3.877	41	3.902	21	0.025
3.906	45	3.944	42	0.038
4.005	58	4.018	16	0.013
4.348	73	4.366	19	0.018
4.383	58	4.404	28	0.021
4.467	76	4.486	17	0.019

of resonance energy. The shifts of barrier resonances are bigger than those of conventional resonances. Compared with the symmetric H + H_2 system,[15,16] for which the 3D resonance energies can be consistently related to the approximate sum of 2D resonance energies and the nearly separable degenerate

TABLE 2: Calculated Energies E_n (eV) and Lifetimes τ_n (fs) of the Transition State Resonances for the Three-Dimensional Mu + H_2 and Mu + D_2 Collisions at Total Angular Momentum $J = 0$

MuH_2		MuD_2	
E_n	τ_n	E_n	τ_n
0.924	5.6	0.883	8.8
1.262	3.8	1.761	9.2
1.605	5.0	1.998	7.6
1.788	6.9	2.280	12
2.072	6.6	2.504	13
2.372	6.0	2.537	31
2.585	18	2.608	25
2.618	23	2.766	8.1
2.703	24	3.038	18
2.752	19	3.083	16
2.814	18	3.275	27
2.867	21	3.320	43
2.910	25	3.360	28
3.305	30	3.432	22
3.344	33	3.475	26
3.404	22	3.512	20
3.430	13	3.722	18
3.450	50	3.772	19
3.491	10	3.798	15
3.558	11	3.823	11
3.601	32	3.906	25
3.626	15	3.967	30
3.671	16	4.052	21
3.706	21	4.113	23
3.745	19	4.156	6.5
3.902	21	4.295	24
3.944	42	4.334	24
4.018	16	4.394	23
4.069	12	4.418	29
4.131	18	4.440	12
4.173	39	4.462	25
4.215	18	4.558	9.8
4.259	38		
4.366	19		
4.404	28		
4.444	18		
4.486	17		
4.544	36		
4.621	17		

TABLE 3: Calculated Energies E_n (eV) and Lifetimes τ_n (fs) of the Transition State Resonances for the Mu + D_2 System[a]

E_n^{2D}	τ_n^{2D}	E_n^{3D}	τ_n^{3D}	ΔE
0.783	7.3	0.883	8.8	0.100
1.654	19	1.761	9.2	0.107
2.473	23	2.504	13	0.031
2.538	24	2.608	25	0.070
3.019	62	3.038	18	0.019
3.230	16	3.275	27	0.045
3.306	32	3.360	28	0.054
3.701	56	3.722	18	0.021
3.872	18	3.906	25	0.024
3.938	77	3.967	30	0.029
4.238	70	4.295	24	0.057
4.368	45	4.394	23	0.026
4.415	115	4.418	29	0.003

[a] The symbols have the meaning given in Table 1.

bends, the Mu + D_2 system exhibits a more intrincate behavior due to its lower symmetry. Thus, for this system, it is difficult to assign the excited resonance states using proper quantum numbers. This is mainly due to the different spacing of the threshold states in the reactant and product channels and to the high resonance energies. In addition, we have noticed that the conventional transition state resonances can be well linked to the reactant and product threshold states. If the difference between a reactant threshold state and a product one is small,

these two states may yield resonances with a near-resonance energy. Finally, we have found that the 3D resonance lifetimes tend to be shorter. Moreover, for both the Mu + H_2 and Mu + D_2 systems, the distributions of lifetimes of resonance states have been found to display a non-RRKM behavior as for the collinear cases.[28]

Summary

We have calculated the energies and widths of transition state resonances of three-dimensional Mu + H_2 and Mu + D_2 collisions using the time-dependent wavepacket propagation method at $J = 0$. Thirty-nine transition state resonances have been reported for Mu + H_2 and 32 for Mu + D_2. Their lifetimes have been found to be shorter than in the 2D case. Finally, it should be pointed out that the present calculations have used only the lowest sheet of the ground state DMBE potential energy surface for H_3, which may be problematic for the high-energy resonance structure. Work to eliminate this limitation and to assign some of the resonance states is clearly desirable.

Acknowledgment. This work has been supported by the Junta Nacional de Investigação Científica e Tecnológica, Portugal, under programs PRAXIS XXI and FEDER (Contract 2/2.1/QUI/408/94).

References and Notes

(1) DeLeon, N.; Mehta, M. A. *Comp. Phys. Rep.* **1988**, *8*, 293.
(2) Truhlar, D. G.; Garrett, B. C. *J. Phys. Chem.* **1992**, *96*, 6515.
(3) Schinke, R. *Photodissociation Dynamics*; Cambridge University Press: Cambridge, U.K., 1993.
(4) Burghardt, I.; Gaspard, P. *J. Chem. Phys.* **1994**, *100*, 6395.
(5) Burghardt, I.; Gaspard, P. *J. Chem. Phys.* **1995**, *99*, 2732.
(6) Mahapatra, S.; Sathyamurthy, N. *J. Chem. Phys.* **1995**, *102*, 6057.
(7) Mahapatra, S.; Sathyamurthy, N.; Kumar, S.; Gianturco, F. A. *Chem. Phys. Lett.* **1995**, *241*, 223.
(8) Heller, E. J. *J. Phys. Chem.* **1995**, *99*, 2625.
(9) Colton, M. C.; Schatz, G. C. *Chem. Phys. Lett.* **1986**, *124*, 256.
(10) Bowman, J. M. *Chem. Phys. Lett.* **1986**, *124*, 260.
(11) Zhang, J. Z. H.; Miller, W. H. *Chem. Phys. Lett.* **1988**, *153*, 465.
(12) Zhao, M.; Mladenovic, M.; Truhlar, D. G.; Schwenke, D. W.; Sharafeddin, O.; Sun, Y.; Kouri, D. J. *J. Chem. Phys.* **1989**, *91*, 5302.
(13) Cuccaro, S. A.; Hipes, P. G.; Kupermann, A. *Chem. Phys. Lett.* **1989**, *157*, 440.
(14) Sadeghi, R.; Skodje, R. T. *J. Chem. Phys.* **1993**, *98*, 9208.
(15) Sadeghi, R.; Skodje, R. T. *J. Chem. Phys.* **1993**, *99*, 5126.
(16) Skodje, R. T.; Sadeghi, R.; Köppel, H.; Krause, J. L. *J. Chem. Phys.* **1994**, *101*, 1725.
(17) Sadeghi, R.; Skodje, R. T. *J. Chem. Phys.* **1995**, *102*, 193.
(18) Sadeghi, R.; Skodje, R. T. *Phys. Rev. A* **1995**, *52*, 1996.
(19) Reid, I. D.; Garner, D. M.; Lee, L. Y.; Senba, M.; Arseneau, D. J.; Fleming, D. G. *J. Chem. Phys.* **1987**, *86*, 5578.
(20) Baer, S.; Fleming, D. G.; Arseneau, D. J.; Senba, M.; Gonzalez, A. *Isotope Effects in Gas-Phase Chemistry*; Kaye, J. A., Ed.; American Chemical Society: Washington, DC, 1992; p 111.
(21) Snooks, R.; Arseneau, D. J.; Fleming, D. G.; Senba, M.; Pan, J. J.; Shelley, M.; Baer, S. *J. Chem. Phys.* **1995**, *102*, 4860.
(22) Bondi, D. K.; Clary, D. C.; Connor, J. N. L.; Garrett, B. C.; Truhlar, D. G. *J. Chem. Phys.* **1982**, *76*, 4986.
(23) Blais, N. C.; Truhlar, D. G.; Garrett, B. C. *J. Chem. Phys.* **1983**, *78*, 2363.
(24) Garrett, B. C.; Truhlar, D. G. *J. Chem. Phys.* **1984**, *81*, 309.
(25) Schatz, G. C. *J. Chem. Phys.* **1985**, *83*, 3441.
(26) Tsuda, K.-i.; Moribayashi, K.; Nakamura, H. *Chem. Phys. Lett.* **1994**, *231*, 439.
(27) Tsuda, K.-i.; Moribayashi, K.; Nakamura, H. *J. Chem. Phys.* **1995**, *103*, 5512.
(28) Varandas, A. J. C.; Yu, H. G. *Chem. Phys.* **1996**, in press.
(29) Varandas, A. J. C.; Brown, F. B.; Mead, C. A.; Truhlar, D. G.; Blais, N. C. *J. Chem. Phys.* **1987**, *86*, 6258.
(30) Feit, M. D.; Fleck, J. A. *Appl. Opt.* **1978**, *17*, 3990.
(31) Feit, M. D.; Fleck, J. A.; Steiger, A. *J. Comput. Phys.* **1982**, *47*, 412.
(32) Tennyson, J.; Sutcliffe, B. T. *J. Chem. Phys.* **1982**, *77*, 4061.
(33) Light, J. C.; Hamilton, I. P.; Lill, J. V. *J. Chem. Phys.* **1985**, *82*, 1400.
(34) Leforestier, C.; Bisseling, R. H.; Cerjan, C.; Feit, M. D.; Friesner, R.; Guldberg, A.; Hammerich, A.; Jolicard, G.; Karrlein, W.; Meyer, H.-D.; Lipkin, N.; Roncero, O.; Kosloff, R. *J. Comput. Phys.* **1991**, *94*, 59.
(35) Neuhauser, D.; Baer, M. *J. Chem. Phys.* **1989**, *90*, 4351.
(36) Press, W. H.; Flannery, B. P.; Teukolsky, S. A.; Vetterling, W. T. *Numerical Recipes*; Cambridge University Press: New York, 1992.
(37) Marple, Jr., S. *Digital Spectral Analysis with Applications*; Prentice-Hall: Englewood Cliffs, NJ, 1987.
(38) Gray, S. K. *J. Chem. Phys.* **1992**, *96*, 6543.
(39) Engel, V. *Chem. Phys. Lett.* **1992**, *189*, 76.

JP9610372